Supporting Information

"Two-in-one" organic-inorganic hybrid Mn^{II} complexes exhibiting dual-emissive phosphorescence

Alexey S. Berezin,[a] Denis G. Samsonenko,[a,b] Valery K. Brel,[c] Alexander V. Artem'ev[a]*

[a]*Nikolaev Institute of Inorganic Chemistry, Siberian Branch of Russian Academy of Sciences, 3, Akad. Lavrentiev Ave., Novosibirsk 630090, Russian Federation*
[b]*Novosibirsk State University, (National Research University), Department of Natural Sciences, 2, Pirogova Str., Novosibirsk 630090, Russian Federation*
[c]*Nesmeyanov Institute of elementorganic compounds of Russian Academy of Sciences, Vavilova st., 28, Moscow, 119991, Russian Federation*
*Author for correspondence: chemisufarm@yandex.ru (Alexander V. Artem'ev)

Table of Contents

Pages

S2-4 X-Ray crystallography

S4-8 Photophysical measurements

S8-10 FT-IR spectra of **1–4**

X-Ray crystallography

Table S1. Data collection and refinement parameters for **1**–**4**.

Compound	**1**·3MeOH	**2**·2MeCN	**3**·2.75MeCN	**4**·3MeOH·2H_2O
CCDC	1576314	1576318	1576317	1576316
Empirical formula	$C_{78}H_{78}Cl_4Mn_2O_9P_6$	$C_{82}H_{78}Br_4Mn_2N_2O_6P_6$	$C_{89.5}H_{80.25}Br_4Mn_2N_{2.75}O_6P_6$	$C_{78}H_{82}Br_2MnO_{11}P_6$
Formula mass [g/mol]	1596.90	1802.80	1905.65	1596.01
Space group	$P2_1/c$	$P2_1$	$P2_1/c$	P-1
a [Å]	13.2413(2)	11.8009(5)	14.9083(3)	12.6473(4)
b [Å]	19.5421(4)	26.2459(8)	28.8164(5)	18.3942(7)
c [Å]	29.2641(6)	13.8906(4)	22.3826(4)	18.4505(4)
α [°]	90.00	90.00	90.00	71.202(3)
β [°]	92.638(2)	111.152(4)	100.5034(18)	83.448(2)
γ [°]	90.00	90.00	90.00	74.079(3)
V [Å^3]	7564.4(2)	4012.4(3)	9454.5(3)	3905.9(2)
Z	4	2	4	2
Crystal size [mm]	0.22 × 0.21 × 0.11	0.48 × 0.21 × 0.13	0.51 × 0.42 × 0.17	0.45 × 0.16 × 0.04
$D_{calcd.}$ [g·cm^{-3}]	1.402	1.492	1.339	1.357
μ [mm^{-1}]	0.658	2.479	2.108	1.372
Temperature [K]	130(2)	130(2)	130(2)	130(2)
Reflections collected	37756	19220	41704	32100
Independent reflections	13807 [R_{int} = 0.0329]	11315 [R_{int} = 0.0212]	18117 [R_{int} = 0.0248]	14790 [R_{int} = 0.0269]
Reflections with $I > 2\sigma(I)$	10957	10383	14271	11991
R_1, wR_2 [$I > 2\sigma(I)$]	0.0565, 0.1416	0.0323, 0.0667	0.0660, 0.1901	0.0421, 0.1104
R_1, wR_2 (all data)	0.0737, 0.1535	0.0382, 0.0694	0.0851, 0.2061	0.0568, 0.1199
Goodness of fit	1.037	1.034	1.043	1.038
Largest diff peak and hole [e/Å^3]	2.61 and -0.52	0.91 and -0.56	2.23 and -1.58	1.13 and -0.63

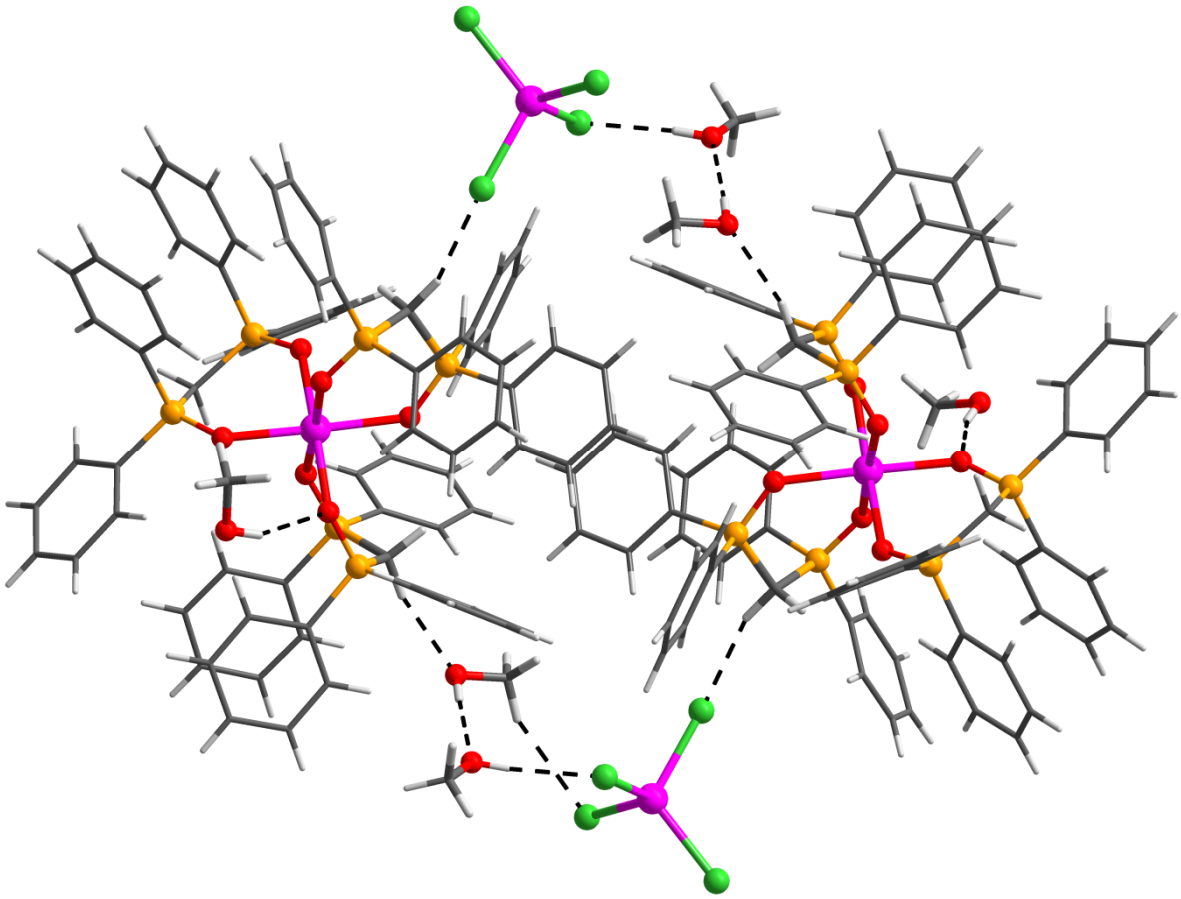

Figure S1. Fragment of the crystal structure of **1**·3MeOH. Hydrogen bonds between $[MnCl_4]^{2-}$ anions and methanol molecules are shown with dashed lines.

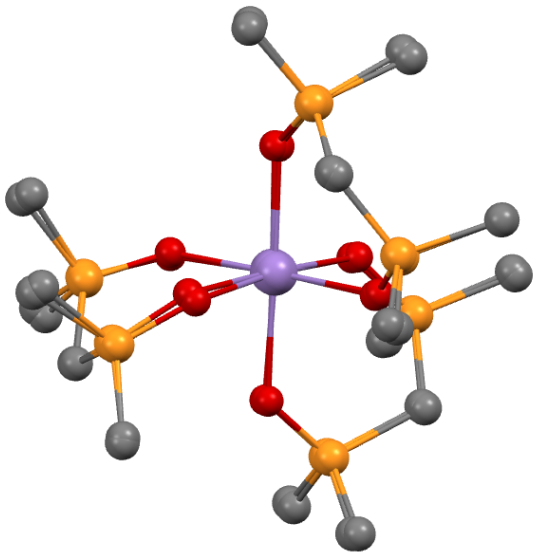

Figure S2. Overlay of the $[Mn(\mathbf{L1})_3]^{2+}$ cations of **1**·3MeOH and **4**·3MeOH·$2H_2O$ (the Ph rings are omitted for clarity).

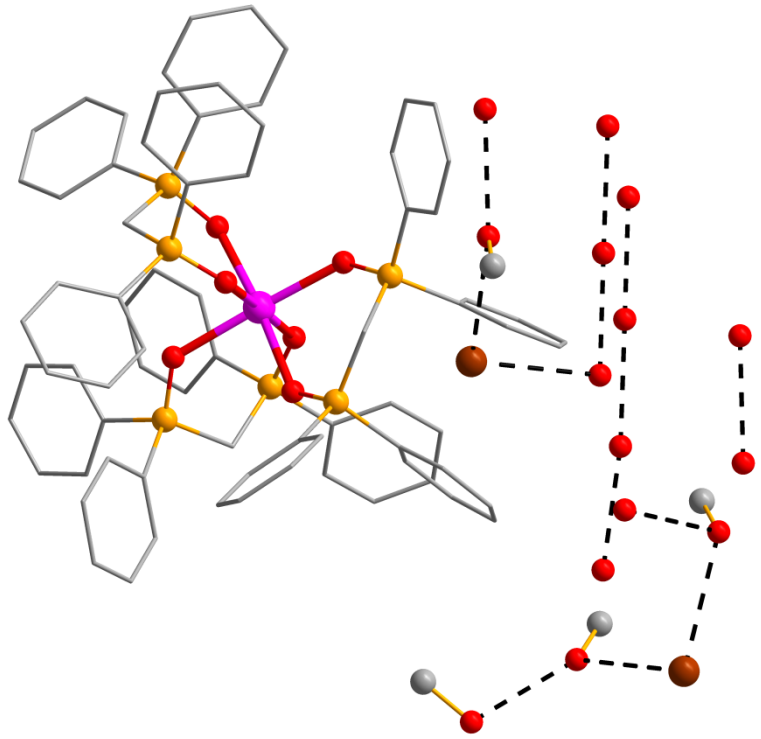

Figure S3. Fragment of the crystal structure of **4**·3MeOH·2H_2O (H atoms are omitted). Hydrogen bonds between bromide anions, disordered water and methanol molecules are shown with dashed lines.

Photophysical measurements

Table S1. Photoluminescence quantum yields (Φ_{em}) of solid-state **1**–**4** at 300 K.

λ_{ex} (nm)	**1**	**2**	**3**	**4**
300	4.6%	12.0%	5.8%	17.0%
440	–	33.7%	49.1%	–
450	–	–	60.7%	–

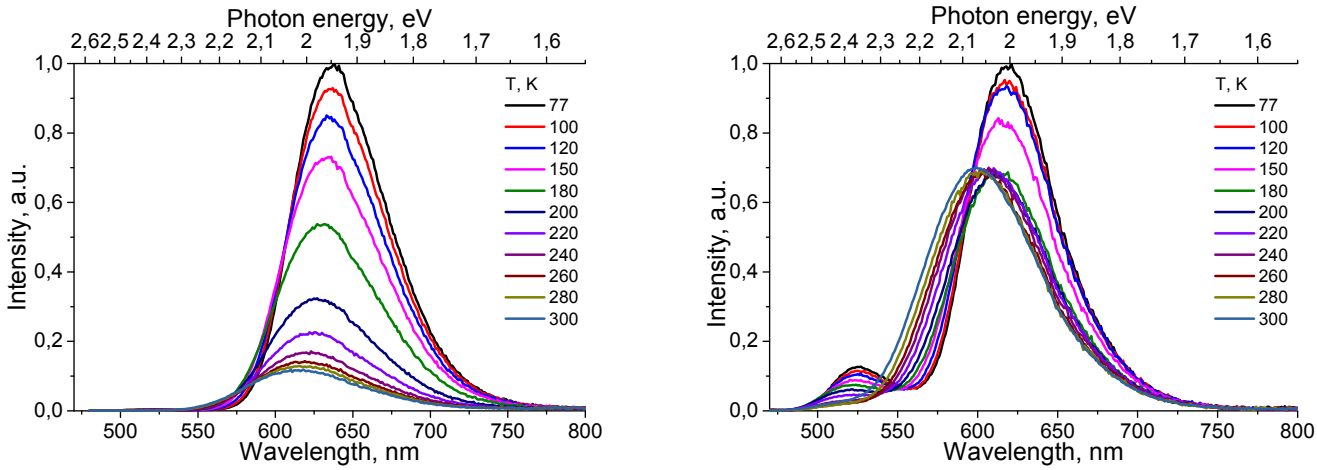

Figure S4. Temperature dependence of solid-state PL spectra of **1** (*left*) and **2** (*right*) with emission at λ_{ex} = 250 nm.

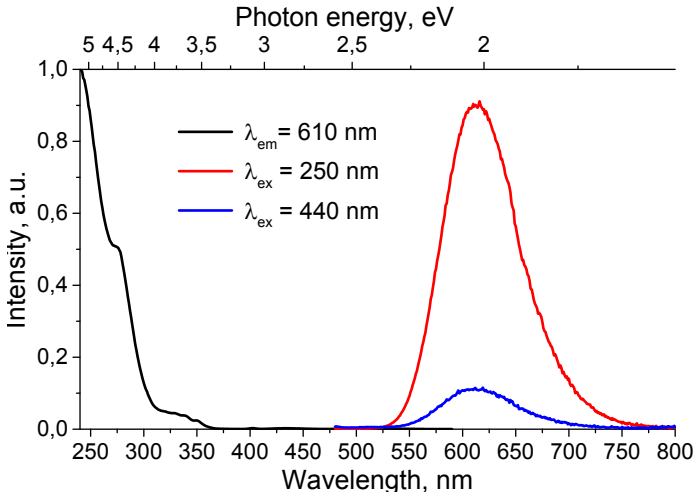

Figure S5. Solid-state PLE and PL spectra of **4**.

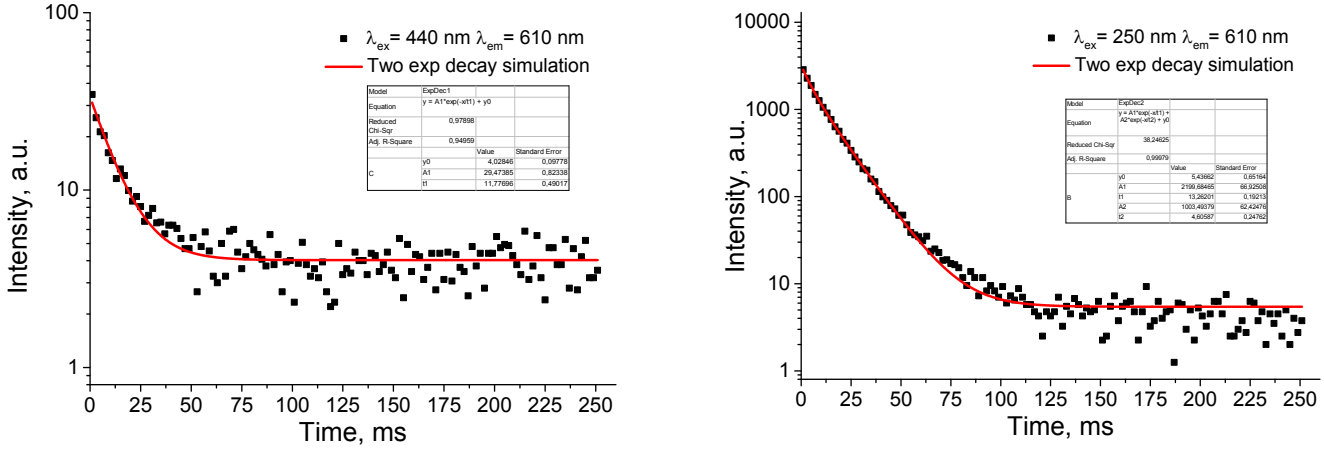

Figure S6. Emission decays for solid complex **1** at 300 K: λ_{ex} = 440 nm and λ_{em} = 610 nm (*left*), λ_{ex} = 250 nm and λ_{em} = 610 nm (*right*).

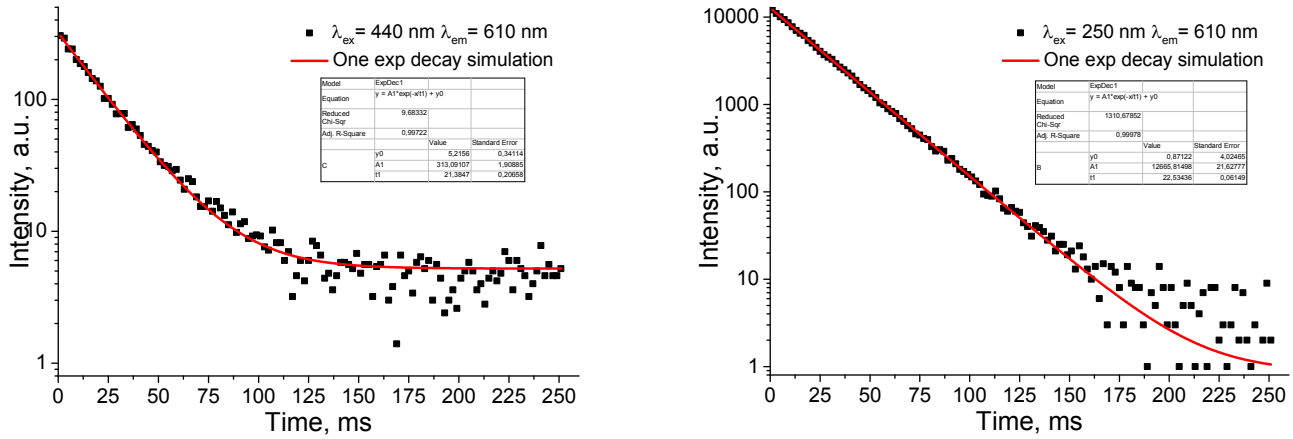

Figure S7. Emission decays for solid complex **2** at 300 K: λ_{ex} = 440 nm and λ_{em} = 610 nm (*left*), λ_{ex} = 250 nm and λ_{em} = 610 nm (*right*).

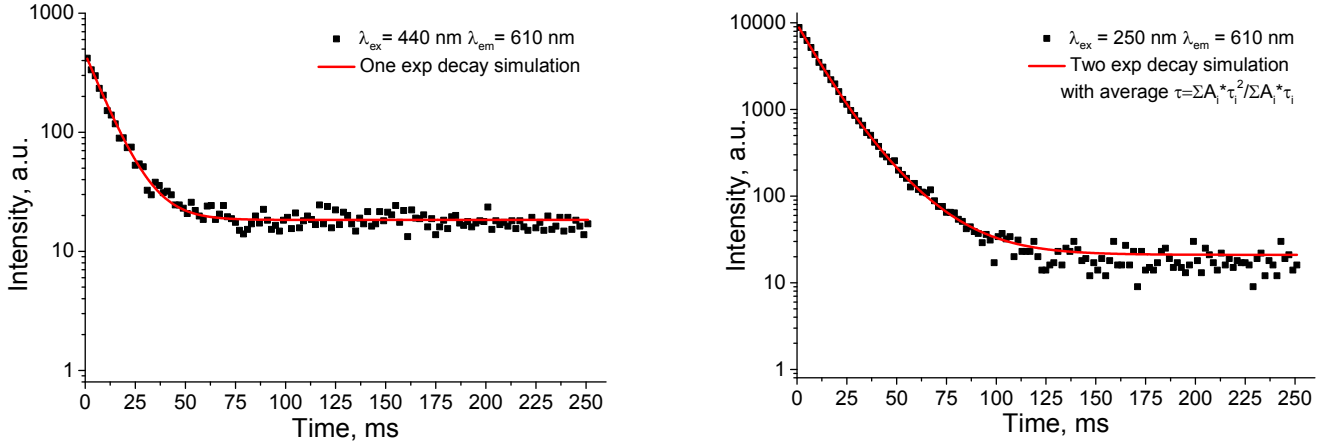

Figure S8. Emission decays for solid complex **3** at 300 K: λ_{ex} = 440 nm and λ_{em} = 610 nm (*left*), λ_{ex} = 250 nm and λ_{em} = 610 nm (*right*).

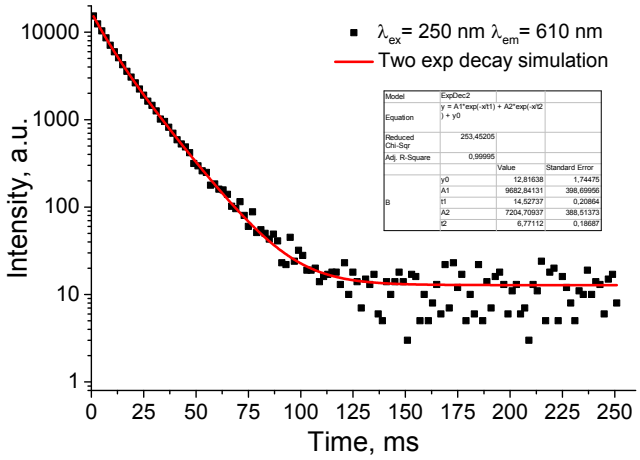

Figure S9. Emission decays for solid complex **4** at 300 K at λ_{ex} = 250 nm and λ_{em} = 610 nm.

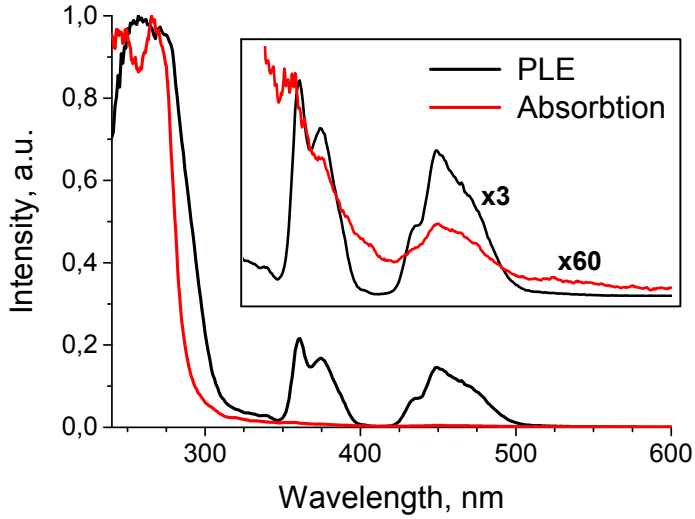

Figure S10. Comparison of solid-state PLE (λ_{em} = 620 nm) and UV–Vis absorption spectra for **3** at 300 K.

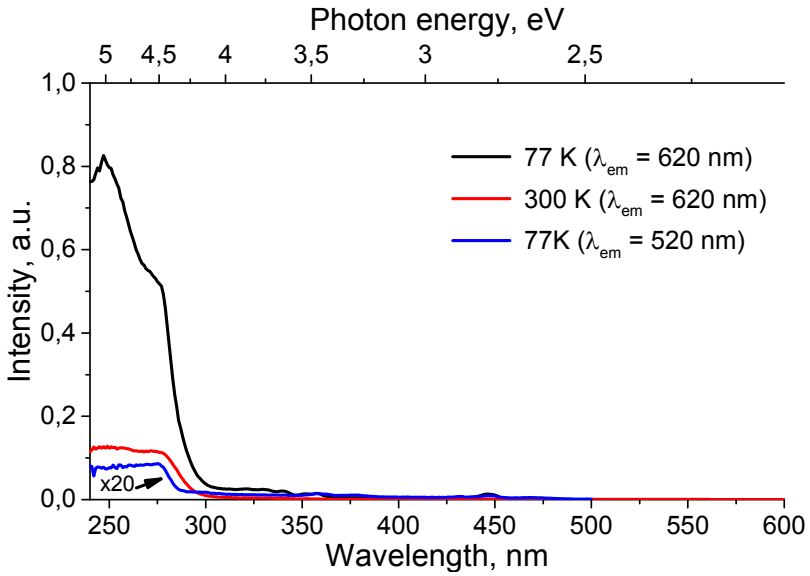

Figure S11. Solid-state PLE spectra of **1** at λ_{em} = 620 and 520 nm at 77 K and 300 K.

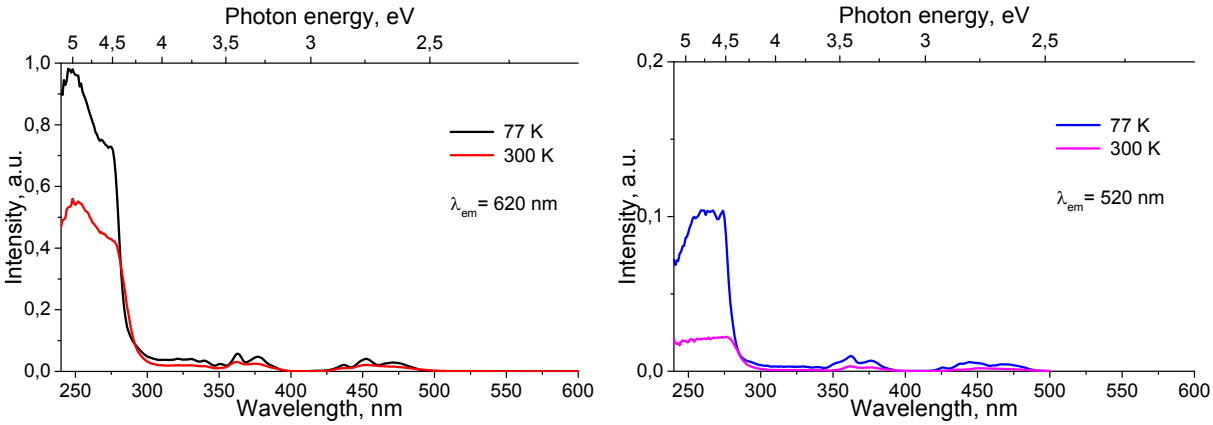

Figure S12. Solid-state PLE spectra of **2** at λ_{em} = 620 nm (*left*) and 520 nm (*right*) at 77 K and 300 K.

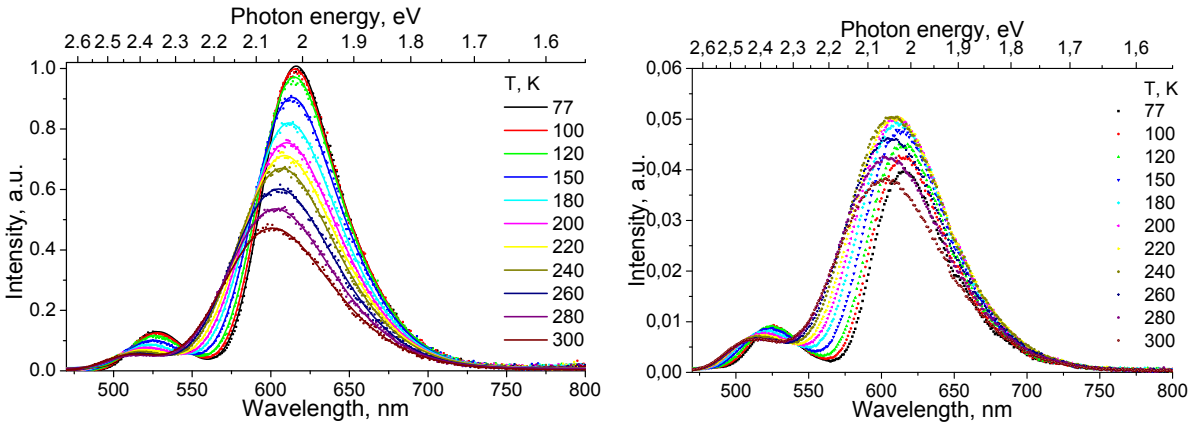

Figure S13. Temperature dependence of solid-state PL spectra of **3** at λ_{ex} = 250 nm (*left*) and λ_{ex} = 440 nm (*right*). Experimental data are presented as scatter, and decomposition by Gauss functions is presented as lines.

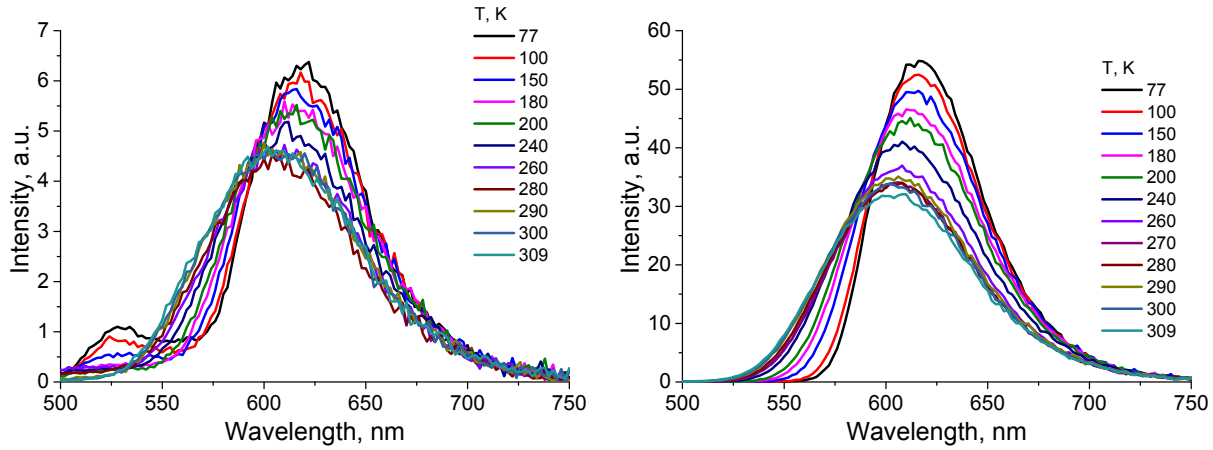

Figure S14. Temperature dependence of time-delayed solid-state PL spectra of **3** at λ_{ex} = 250 nm: 0.1–1 ms (*left*) and 1–10 ms (*right*).

FT-IR spectra of 1–4

Figure S15. FT-IR spectrum of [Mn(**L1**)$_3$]MnCl$_4$ (**1**).

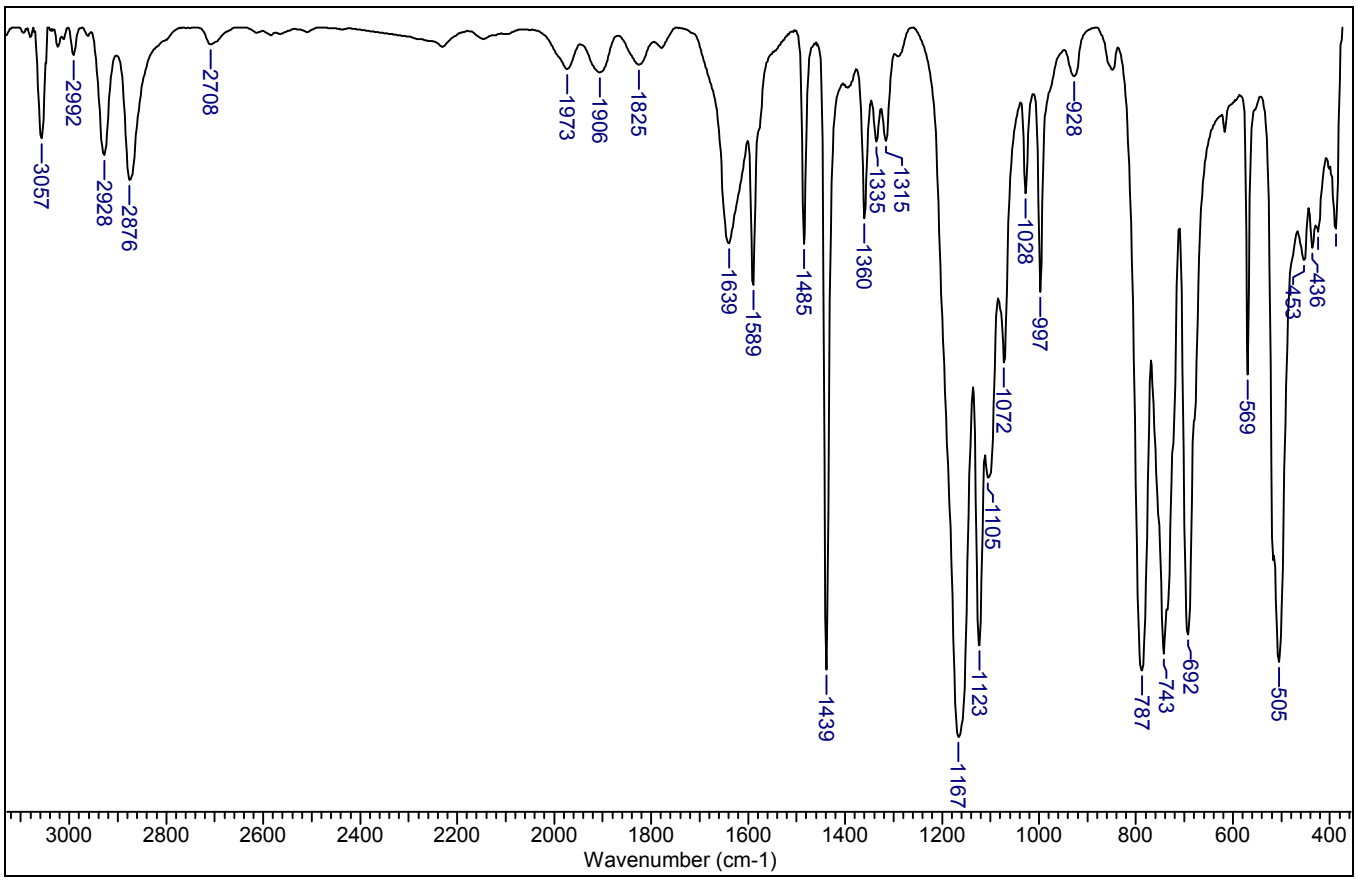

Figure S16. FT-IR spectrum of $[Mn(\mathbf{L2})_3]MnBr_4$ (**2**).

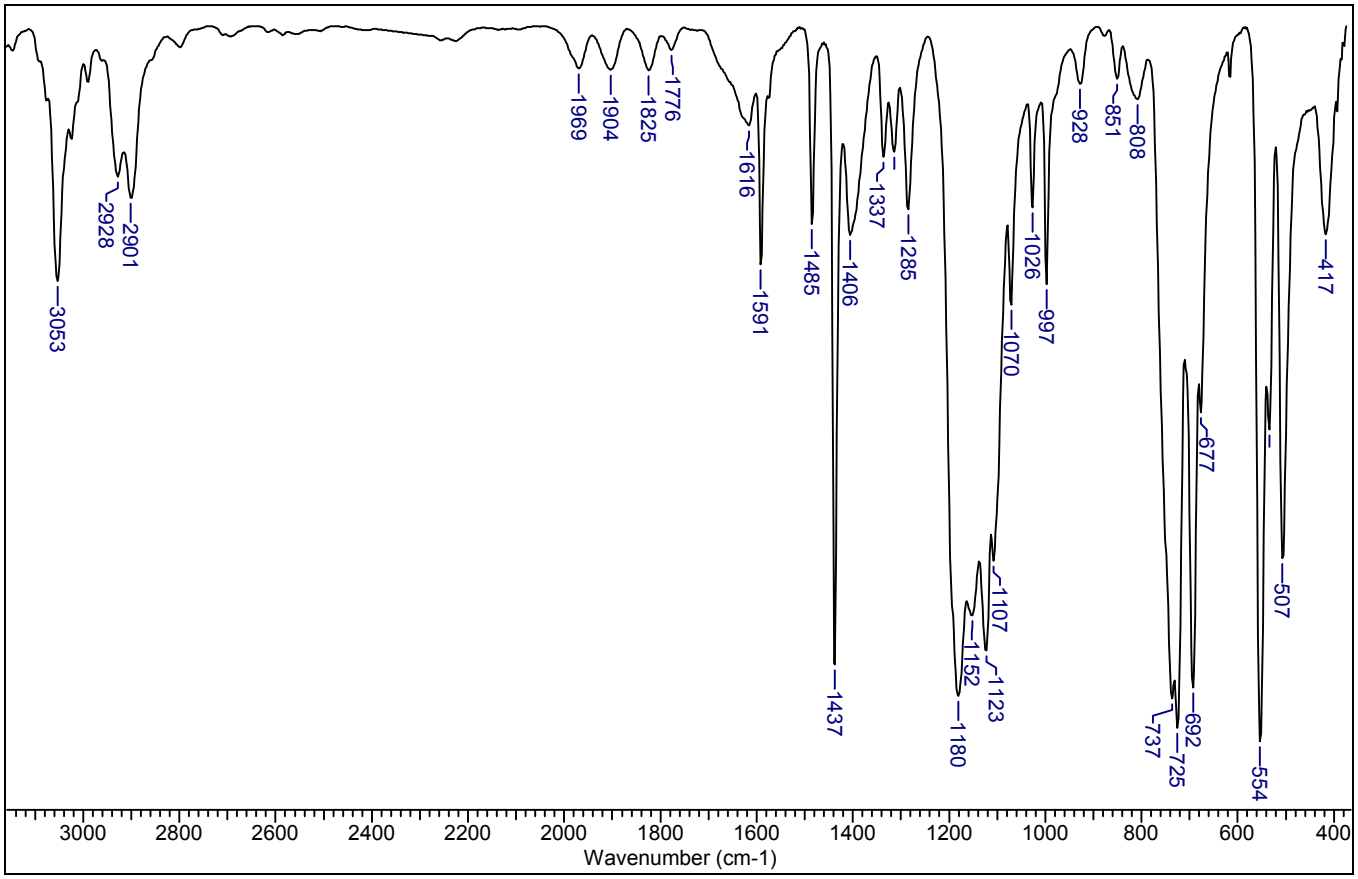

Figure S17. FT-IR spectrum of $[Mn(\mathbf{L3})_3]MnBr_4$ (**3**).

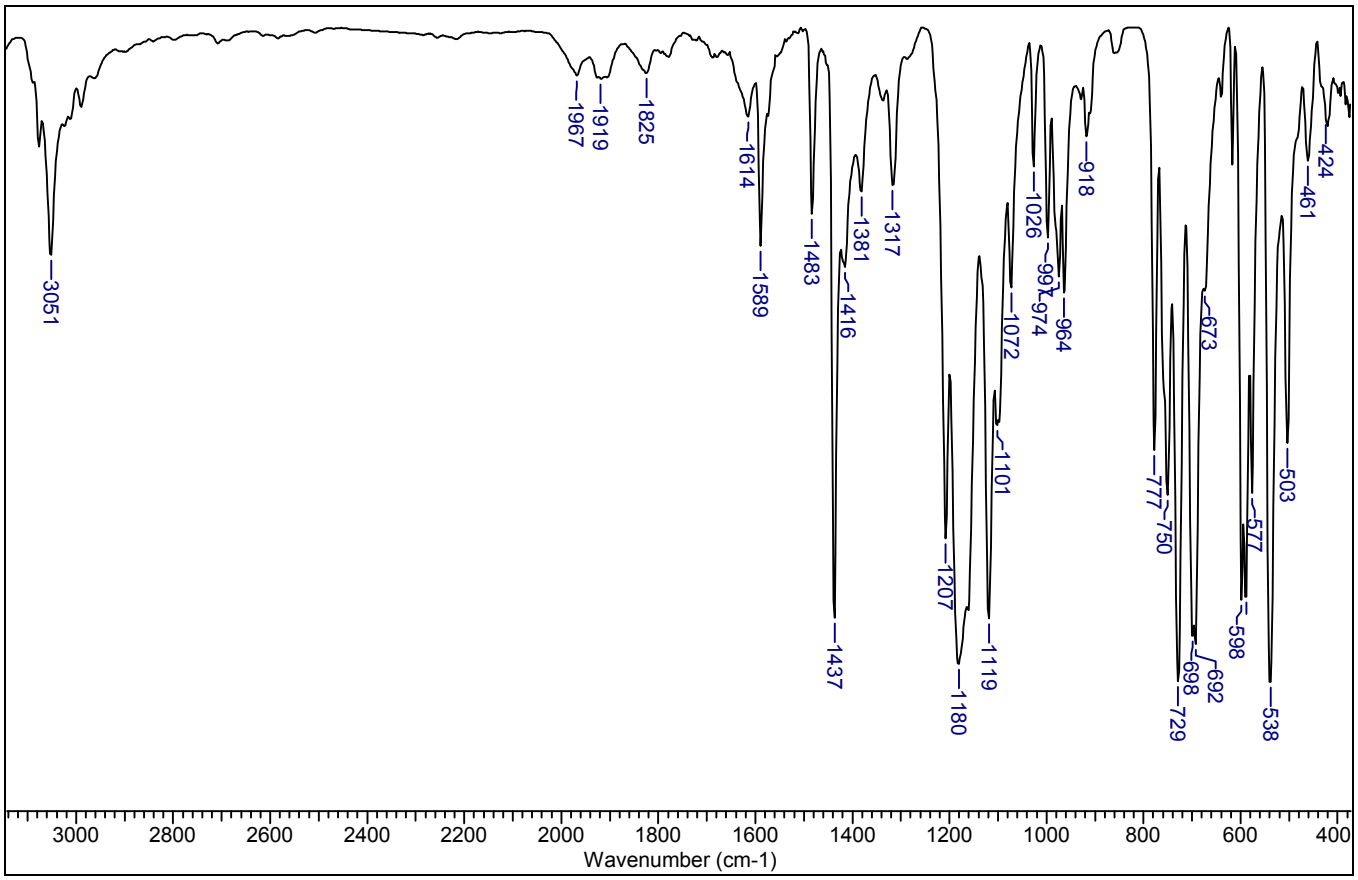

Figure S18. FT-IR spectrum of $[Mn(\mathbf{L1})_3]Br_2$ (**4**).